Lithium Ion Conductors

DOI: 10.1002/anie.200703900

Li_6PS_5X: A Class of Crystalline Li-Rich Solids With an Unusually High Li^+ Mobility**

Hans-Jörg Deiseroth, Shiao-Tong Kong, Hellmut Eckert, Julia Vannahme, Christof Reiner, Torsten Zaiß, and Marc Schlosser*

The mineral argyrodite (Ag_8GeS_6) was the first representative of a group of solids known as argyrodites[1,2] that are characterized, in general, by a high ionic conductivity and mobility of their Ag^+ ions. The structural and conductivity data of these compounds have been called on repeatedly to explain these physical properties in light of the complex argyrodite structure type.[3–18] These studies have improved the general understanding of the diffusion paths of the mobile ions as a function of the temperature and structural properties. The Ag^+ ions in these compounds can be substituted by other cations, usually Cu^+, and versatile substitution reactions of P and S whilst maintaining the topology of the argyrodite structure have also been reported.

Considering the great interest in the mobility of Li^+ ions in solids it was surprising to us that there are only a few reports of experimental work with the corresponding crystalline Li analogues, and none of these appear to be aware of, or even mention, the argyrodite connection. One of these papers reports the synthesis of a black powder containing Li_7PS_6 and $Li_8P_2S_9$ (minority phase),[19] and another gives detailed NMR-spectroscopy-based information on the behavior of Li^+ ions in a series of pre-reacted amorphous and crystalline mixtures of Li_2S and P_2S_5.[20] A few papers have been published on the application of glass ceramics obtained by high-energy milling of Li_2S/P_2S_5 mixtures and their application in secondary batteries in recent years[21–23] although, again the possible argyrodite connection, is not mentioned. Thus, well-established syntheses of crystalline single-phase Li argyrodites and reliable structural and physical data are not available.

Although there is some controversy about the radii of the univalent cations of Group 11,[24] it can be assumed that the radii of Cu^+ and Li^+ are quite similar and different to Ag^+ ($Cu^+ = 74$ pm, $Li^+ = 73$ pm, $Ag^+ = 114$ pm; all coordination number(CN) = 4). This situation clearly favors a partial or full mutual substitution of Li^+ and Cu^+ ions in argyrodites and thus the existence of synthetic "Li-argyrodites". The enhanced reactivity of elemental Li and its compounds at higher temperatures compared to Ag and Cu, however, requires special precautions concerning appropriate container materials and may be the reason for this apparent knowledge gap.

The crystal structures of the high-temperature phases of argyrodites are based on a tetrahedral close packing of the nonmetal atoms (chalcogen/halogen) following the topology of a cubic Laves phase (e.g., $MgCu_2$). The 24 chalcogen atoms in the unit cell of Ag_9AlSe_6 ($Z = 4$[12]) form 136 tetrahedral holes which are occupied by four Al^{3+} (ordered) and 36 Ag^+ ions. These Ag^+ ions are dynamically and/or statically disordered, which explains the high Ag^+ (Cu^+) ionic conductivities of many argyrodites.

Li_6PS_5X (X: Cl, Br, I) represents a series of argyrodites whose chemical formula is based on a well-known substitution pattern for the corresponding Ag and Cu compounds characterized by the replacement of one chalcogen by one halogen atom with S and X atoms ordered on separate crystallographic positions. Consequently, this substitution requires only six Li atoms per formula unit instead of seven. According to the structure of Ag_9AlSe_6, the P atoms of Li_6PS_5X are expected to fill four of the 136 tetrahedral holes formed by S atoms only (S1) but distributed in such a way that the PS_4 tetrahedra do not share common S1 atoms. The remaining 132 tetrahedral holes (formed by S2 and X) are partially occupied in a disordered manner by significantly off-centered Li^+ ions, which results in the ionic formula $(Li^+)_6(PS_4^{3-})S^{2-}X^-$ (Figure 1a). It is very likely that the Li^+ positions are similar to those found for Ag/Cu in the corresponding Ag and Cu argyrodites, although the locations of individual Li^+ ions remain to a certain extent speculative (see below) because of the low visibility of these ions as a result of their presumed random distribution and low scattering power. The randomly occupied atomic positions 48*h* and 24*g* of space group $F\bar{4}3m$ play a key role in the diffusion paths of mobile cations in all argyrodites, as demonstrated previously for similar Ag and Cu compounds. These positions have the strongest occupancies in a complex three-dimensional diffusion pattern (described in detail elsewhere)[8,10,12,18] and are typically involved when Cu/Ag ions jump through the common face of two adjacent tetrahedral holes. Both these positions could be refined significantly for the title compounds but with high standard deviations.

[*] Prof. Dr. H.-J. Deiseroth, M.Sc. S.-T. Kong, Dr. C. Reiner, Dr. T. Zaiß, Dr. M. Schlosser
Anorganische Chemie
Universität Siegen
Adolf-Reichwein-Strasse 2, 57068 Siegen (Germany)
Fax: (+49) 271-740-2555
E-mail: deiseroth@chemie.uni-siegen.de
Homepage: http://www.uni-siegen.de/fb8/ac/
Prof. Dr. H. Eckert, Dr. J. Vannahme
Institut für Physikalische Chemie
Westfälische Wilhelms-Universität Münster
Corrensstrasse 30/36, 48149 Münster (Germany)

[**] We gratefully acknowledge continuing support by the Deutsche Forschungsgemeinschaft and the Fonds der Chemischen Industrie. H.E. and J.V. acknowledge funding by the Deutsche Forschungsgemeinschaft through the SFB 458 program. We would also like to thank Prof. Dr. H.-D. Wiemhöfer (WWU Münster) for performing the impedance measurements. X = Cl, Br, I.

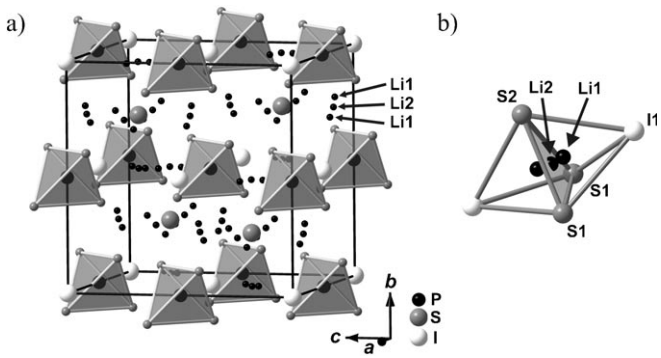

Figure 1. a) A section of the crystal structure of Li_6PS_5I showing the distribution of PS_4 tetrahedra and single S^{2-} (S2, in four octants of the cell) and I^- ions (corners and faces of the cell). b) A face-sharing S_3I_2 double tetrahedron containing Li1 (above and below the common face) and Li2 (center of the common face).

Position 24*g* (Li2) is located in the center of the common triangular face whereas 48*h* (Li1) represents two closely neighboring positions ($d_{Li1-Li1}$ is approximately 115 pm for Li_6PS_5I) above and below 24*g* that are shifted slightly towards the centers of the connected tetrahedra (Figure 1b). Simultaneous occupation of these positions is excluded, although difference-Fourier syntheses clearly show low but significant electron densities (approx. 1 e Å^{-3}) for all three positions. The expected electron densities for the other positions of the diffusion paths are less than 1 e Å^{-3}.

Preliminary impedance measurements at room temperature show promising specific Li-ion conductivities in the range 10^{-2} to 10^{-3} S cm^{-1}, and thus support the single-crystal results. More detailed information about the lithium-ion dynamics, however, is currently only available from the static ^{7}Li NMR spectroscopy measurements summarized in Figure 2.

The ^{7}Li NMR line-shapes in the low-temperature range (140–160 K) are governed by strong homonuclear ^{7}Li–^{7}Li magnetic dipole–dipole interactions, which result in static linewidths of around 6000 Hz for the iodide and chloride compounds. The lines sharpen dramatically as the temperature is increased, thereby indicating the onset of motional narrowing. Figure 2 clearly shows that the narrowing effect occurs at particularly low temperatures for Li_6PS_5Br (the rigid linewidth is not reached at 140 K, which is the lowest accessible temperature, and the line-narrowing process is completed at 200 K). These results indicate that Li_6PS_5Br has the highest lithium-ion mobility amongst the title compounds. Furthermore, the temperature-dependent linewidths for the iodide compound reveal an interesting two-step narrowing behavior, which suggests a more restricted motion at intermediate temperatures (170–250 K). It is interesting to note that this intermediate motional process is only observed in the iodide compound, where S^{2-} and I^- are structurally ordered, and is not observed in the two other compounds where sulfide and halide ions are structurally disordered (see below).

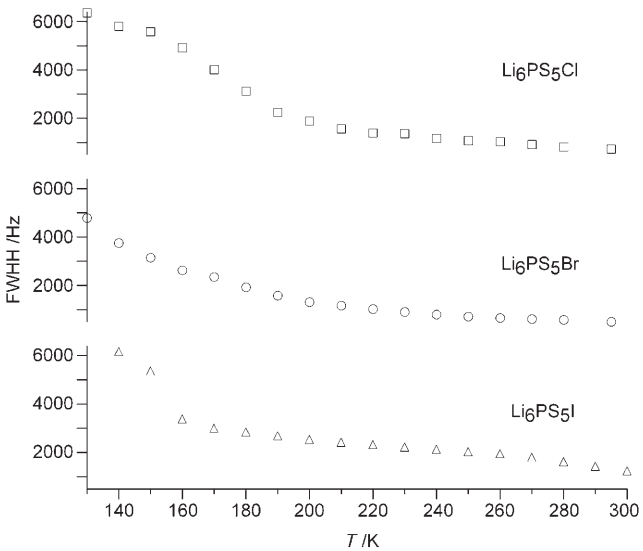

Figure 2. Static ^{7}Li NMR full widths at half height for Li_6PS_5Cl, Li_6PS_5Br, and Li_6PS_5I as a function of temperature.

The halide atoms in most halide-substituted argyrodites occupy a separate crystallographic position that means they avoid direct contact with P (or the respective Group 13, 14, or 15 atom). This is also true for Li_6PS_5I, according to the single-crystal X-ray measurements, but not for Li_6PS_5Br or Li_6PS_5Cl (Figure 3), where the NMR spectroscopy and single-crystal results give clear evidence for a distribution of Cl^-, Br^-, and S^{2-} ions over three crystallographic positions. While the extent of substitution of halide in the S1 sites is small (less than 2% in the case of Li_6PS_5Br), there is substantial occupational mixing of sulfide and halide in the S2 and X

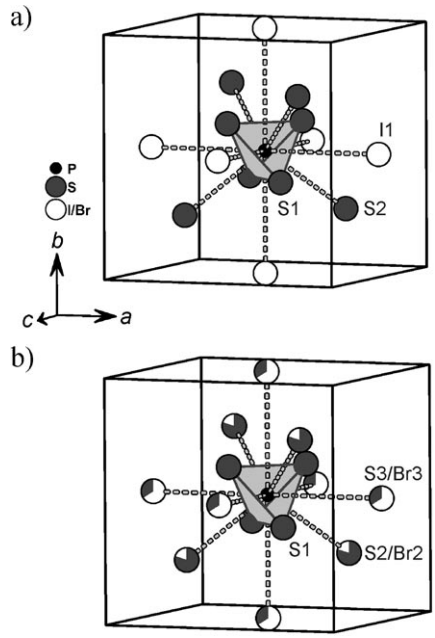

Figure 3. A section of the crystal structure of Li_6PS_5X showing the coordination around phosphorus and the mutual substitution of S and Br/Cl on the respective crystallographic positions. a) Li_6PS_5I: S1, S2, and I ordered without any significant mutual substitution. b) Li_6PS_5Br: minor substitution (1–2%) of S1 by Br (not shown), mutual substitution of S and Br on the S2 site (84% S, 16% Br) and on the X site (40% S, 60% Br). No quantitative information can be given for Li_6PS_5Cl (see text).

sites. The single-crystal analysis for Li_6PS_5Br reveals occupancies of 84% S and 16% Br at the S2 site and 60% Br and 40% S at the X site. No quantitative populations can be given for Li_6PS_5Cl owing to the small X-ray contrast for S and Cl.

Figure 4 shows the ^{31}P magic-angle spinning (MAS)-NMR spectra obtained for powdered materials and reveals striking differences in their general spectral appearance. Thus, while the ^{31}P MAS-NMR spectrum of Li_6PS_5I is very sharp and well-defined, that of Li_6PS_5Cl is extremely broad, thereby indicating a number of poorly resolved contributions. Most interestingly, the ^{31}P MAS-NMR spectrum of Li_6PS_5Br seems to show both a sharp and a broad component, with the latter again consisting of several contributions. An analogous behavior is seen for the halide resonances (Figure 5). Both Figures 4 and 5 indicate that the iodide phase appears to be fully ordered, the chloride phase fully disordered, and the sample of Li_6PS_5Br consists of both ordered and disordered crystallites or domains.

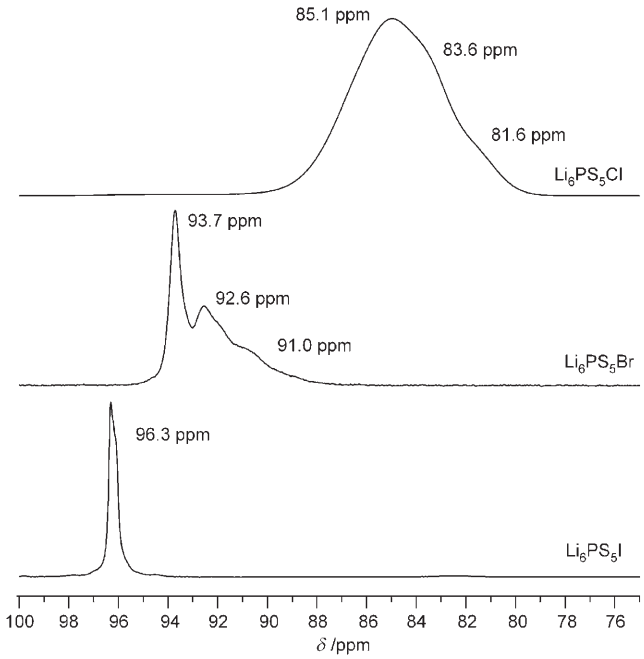

Figure 4. ^{31}P MAS-NMR spectra of Li_6PS_5Cl, Li_6PS_5Br, and Li_6PS_5I.

The ordered part of the ^{79}Br NMR spectrum shows a well-defined sharp resonance and spinning sideband manifold at $\delta = 109$ ppm (25% of the total area), whereas the disordered part shows a broader signal at $\delta = -40$ ppm (75% of the total intensity). The sharp line at $\delta = 93.7$ ppm (27 ± 2% of the total area) in the ^{31}P MAS-NMR spectrum of this compound can be assigned to the crystallographically ordered domains, while the broader resonances at lower frequencies (73 ± 2% of the total intensity) can be assigned to the PS_4^{3-} units in the disordered part of the sample that shows a distribution of the bromide ion over the S/Br2 and S/Br3 positions. This disordering effect produces multiple environments for the PS_4^{3-} groups depending on whether their four second nearest neighbors are four S atoms, three S atoms, and one halide, or two S atoms and two halides (see Figure 3). Additional multiplicities may arise from S^{2-}/Br^- ion distribution effects over the six positions in the third coordination sphere.

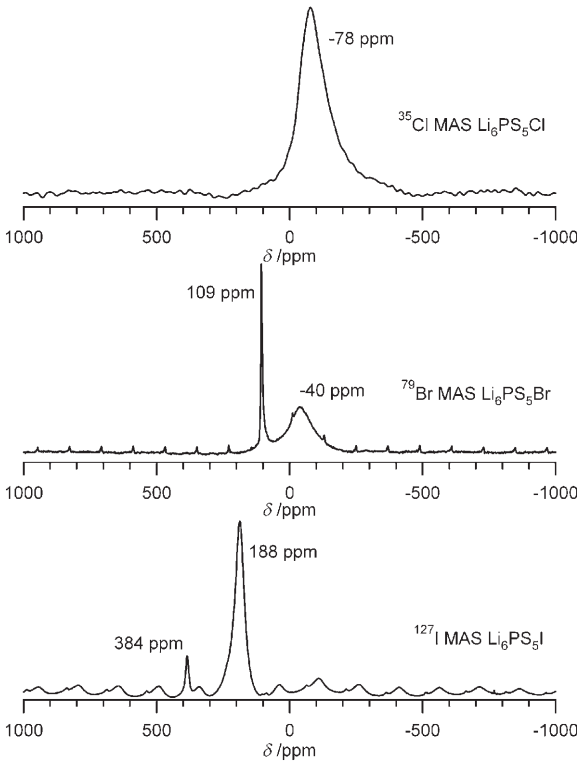

Figure 5. ^{35}Cl, ^{79}Br, and ^{127}I MAS-NMR spectra of Li_6PS_5Cl, Li_6PS_5Br, and Li_6PS_5I. Minor peaks are spinning sidebands. The resonance at $\delta = 384$ ppm in the ^{127}I spectrum is probably due to an impurity.

Finally, the NMR spectra confirm that the extent of halide occupancy in the S1 position is very low, as suggested by the X-ray analysis. If minor amounts of PS_3Br^{2-} or PS_3Cl^{2-} ions were present, these species would give rise to separate low-intensity resonances. Although such low-intensity signals can indeed be identified at $\delta = 102$ and 95 ppm for Li_6PS_5Br and Li_6PS_5Cl, respectively, we cannot exclude that they arise from low levels of impurities in the samples. It is very likely that the preferred substitution of S^{2-} by Br^-/Cl^- ions rather than I^- ions can be rationalized by a comparison of the ionic radii, which are similar for the pair Cl^-/S^{2-} (Cl^-: 181 pm; S^{2-}: 184 pm), moderately different for Br^-/S^{2-} (Br^-: 196 pm), but significantly different for I^-/S^{2-} (I^-: 220 pm).

Experimental Section

Crystalline samples of the colorless, air-sensitive Li-argyrodites Li_6PS_5X (X: Cl, Br, I) were prepared by the reaction of stoichiometric mixtures of Li_2S,[25] P_2S_5 (Acros, 98+%), and LiX (Fluka, p. a.). The starting materials were intimately mixed under inert gas (Ar, < 1 ppm H_2O, < 1 ppm O_2), pressed into pellets, and subsequently heated to 550°C for 7 days. Standard X-ray powder diagrams did not show contamination by any other phases. Single crystals were selected in a glove box equipped with a microscope and transferred into X-ray capillaries, which were subsequently sealed. The single-crystal X-ray measurements were performed with a STOE IPDS diffractometer.[26]

^7Li, ^{31}P, and ^{35}Cl NMR spectroscopy studies were performed with a Bruker DSX 400 spectrometer at operating frequencies of 155.45,

161.92, and 39.19 MHz, respectively. Static, variable-temperature ^{7}Li NMR spectra were recorded for samples enclosed in sealed glass ampoules over the temperature range 140–300 K; temperatures were adjusted with a flow of nitrogen gas controlled by a Bruker VT 3000 heating unit. Static ^{7}Li NMR spectra were measured with an echo sequence (45°–30 μs–90°–20 μs) using relaxation delays of between 1 and 10 s. ^{31}P MAS-NMR spectra were recorded in the single-pulse mode at a spinning speed of 15 kHz with a typical 90° pulse length of 2 μs and a relaxation delay of 60 s. ^{35}Cl MAS-NMR spectra were recorded at a spinning speed of 14 kHz, using 4.5-μs pulses and a relaxation delay of 0.1 s. ^{79}Br and ^{127}I MAS-NMR measurements were performed with a Bruker DSX 500 NMR spectrometer operating at frequencies of 125.3 and 100.1MHz, respectively. Spectra were recorded at a spinning speed of 15 kHz, using 1-μs (2-μs) pulses and a relaxation delay of 1 s. Chemical shifts are reported relative to 1M aqueous solutions of LiCl, KBr, and KI and to 85% H_3PO_4, respectively.

Received: August 24, 2007
Revised: October 11, 2007

Keywords: argyrodites · conducting materials · halides · lithium · NMR spectroscopy

[1] A. Weisbach, *Neues Jahrb. Mineral.* **1886**, *2*, 67–71.
[2] C. Winkler, *Ber. Dtsch. Chem. Ges.* **1886**, *19*, 210–211.
[3] S. Geller, *Z. Kristallogr.* **1979**, *149*, 31–47.
[4] B. Krebs, J. Mandt, *Z. Naturforsch. B* **1977**, *32*, 373–379.
[5] W. F. Kuhs, R. Nitsche, K. Scheunemann, *Acta Crystallogr. Sect. B* **1978**, *34*, 64–70.
[6] W. F. Kuhs, R. Nitsche, K. Scheunemann, *Mater. Res. Bull.* **1979**, *14*, 241–248.
[7] E. E. Hellstrom, R. A. Huggins, *J. Solid State Chem.* **1980**, *35*, 207–214.
[8] F. Boucher, M. Evain, R. Brec, *J. Solid State Chem.* **1993**, *107*, 332–346.
[9] H. Wada, M. Ishii, M. Onoda, M. Tansho, A. Sato, *Solid State Ionics* **1996**, *86–88*, 159–163.
[10] M. Evain, E. Gaudin, F. Boucher, V. Petricek, F. Taulelle, *Acta Crystallogr. Sect. B* **1998**, *54*, 376–383.
[11] E. Gaudin, F. Boucher, V. Petricek, F. Taulelle, M. Evain, *Acta Crystallogr. Sect. B* **2000**, *56*, 402; E. Gaudin, F. Boucher, V. Petricek, F. Taulelle, M. Evain, *Acta Crystallogr. Sect. B* **2000**, *56*, 972–979.
[12] E. Gaudin, H. J. Deiseroth, T. Zaiß, *Z. Kristallogr.* **2001**, *216*, 39–44.
[13] R. Belin, L. Aldon, A. Zerouale, C. Belin, M. Ribes, *Solid State Sci.* **2001**, *3*, 251–256.
[14] R. B. Beeken, J. J. Garbe, J. M. Gillis, N. R. Petersen, B. W. Podoll, M. R. Stoneman, *J. Phys. Chem. Solids* **2004**, *66*, 882–886.
[15] T. Nilges, A. Pfitzner, *Z. Kristallogr.* **2005**, *220*, 281–294.
[16] A. Gagor, A. Petraszko, D. Kaynts, *J. Solid State Chem.* **2005**, *178*, 3366–3375.
[17] R. Blachnik, U. Wickel, *Z. Naturforsch. B* **1980**, *35*, 1268–1271.
[18] T. Zaiß, H. J. Deiseroth, *Z. Kristallogr. New Cryst. Struct.* **2006**, *221*, 119.
[19] J. F. Brice, *C. R. Acad. Sci. Ser. IIc* **1976**, *283*, 581–584.
[20] H. Eckert, Z. Zhang, J. H. Kennedy, *Chem. Mater.* **1990**, *2*, 273–279.
[21] F. Mizuno, A. Hayashi, K. Tadanaga, M. Tatsumisago, *Electrochem. Solid-State Lett.* **2005**, *8*, A603–A606.
[22] F. Mizuno, A. Hayashi, K. Tadanaga, M. Tatsumisago, *J. Power Sources* **2005**, *146*, 711–714.
[23] M. Fuminon, H. Akitoshi, M. Tatsumisago, *Solid State Ionics* **2006**, *177*, 2721–2725.
[24] M. S. Liao, W. H. E. Schwarz, *Acta Crystallogr. Sect. B* **1994**, *50*, 9–12.
[25] K. Yamamoto, N. Ikeda (Furukawa CO LTD), EP-0802159, **1997**.
[26] Crystal structure data for Li_6PS_5Cl: $M_r = 268.36$, STOE IPDS, $T = 296(2)$ K, $Mo_{K\alpha}$ ($\lambda = 71.073$ pm), $2\theta_{max} = 60.62°$, crystal size $0.15 \times 0.08 \times 0.06$ mm^3, cubic, space group $F\bar{4}3m$ (no. 216), $a = 985.9(2)$ pm, $V = 0.9581(4)$ nm^3, $Z = 4$, $\rho_{calcd} = 1.860$ g cm^{-1}, $\mu(Mo_{K\alpha}) = 1.570$ mm^{-1}, 2092 measured reflections, 181 of which are independent, $R_{int} = 0.0601$, least-squares refinement (all atoms anisotropic except for Li1; Li2 could not be refined) on F^2 (G. M. Sheldrick, SHELXL-97, program for the refinement of crystal structures, Universität Göttingen, Germnay, **1997**); numerical absorption correction on the basis of crystal description with 12 faces, (X-RED 1.19, STOE & Cie, **1999**), min./max. transmission factor 0.8856/0.9257, Flack parameter $\eta = 0.021(13)$, R values (all data/($F_0^2 \geq 2\sigma(F_0^2)$)) $R_1 = 0.0544/0.0367$, $wR_2 = 0.0993/0.0919$, GooF = 1.066 for 140 observed reflections ($F_0^2 \geq 2\sigma(F_0^2)$) and 12 refined parameters. Crystal structure data for Li_6PS_5Br: $M_r = 312.82$, STOE IPDS, $T = 296(2)$ K, $Mo_{K\alpha}$ ($\lambda = 71.073$ pm), $2\theta_{max} = 60.92°$, crystal size $0.28 \times 0.11 \times 0.11$ mm^3, cubic, space group $F\bar{4}3m$ (no. 216), $a = 998.8(2)$ pm, $V = 0.9963(4)$ nm^3, $Z = 4$, $\rho_{calcd} = 2.085$ g cm^{-1}, $\mu(Mo_{K\alpha}) = 5.253$ mm^{-1}, 1433 measured reflections, 183 of which are independent, $R_{int} = 0.0571$, least-squares refinement (all atoms anisotropic except Li) on F^2 (SHELXL-97); numerical absorption correction on the basis of crystal description with seven faces (X-RED), min./max. transmission factor 0.5252/0.6930, Flack parameter $\eta = 0.009(5)$, R values (all data/($F_0^2 \geq 2\sigma(F_0^2)$)) $R_1 = 0.0441/0.0311$, $wR_2 = 0.0750/0.0693$, GooF = 1.031 for 151 observed reflections ($F_0^2 \geq 2\sigma(F_0^2)$) and 18 refined parameters. Crystal structure data for Li_6PS_5I: $M_r = 359.81$, STOE IPDS, $T = 296(2)$ K, $Mo_{K\alpha}$ ($\lambda = 71.073$ pm), $2\theta_{max} = 60.68°$, crystal size $0.23 \times 0.06 \times 0.05$ mm^3, cubic, space group $F\bar{4}3m$ (no. 216), $a = 1014.5(2)$ pm, $V = 1.0441(3)$ nm^3, $Z = 4$, $\rho_{calcd} = 2.289$ g cm^{-1}, $\mu(Mo_{K\alpha}) = 4.143$ mm^{-1}, 2315 measured reflections, 195 of which are independent, $R_{int} = 0.0419$, least-squares refinement (all atoms anisotropic except Li) on F^2 (SHELXL-97); numerical absorption correction on the basis of a crystal description with seven faces (X-RED), min./max. transmission factor 0.6259/0.8205, Flack parameter $\eta = -0.035(5)$, R values (all data/($F_0^2 \geq 2\sigma(F_0^2)$)) $R_1 = 0.0257/0.0230$, $wR_2 = 0.0516/0.0503$, GooF = 1.103 for 178 observed reflections ($F_0^2 \geq 2\sigma(F_0^2)$) and 15 refined parameters. Further details of the crystal structure investigations may be obtained from the Fachinformationszentrum Karlsruhe, 76344 Eggenstein-Leopoldshafen, Germany (fax: (+49) 7247-808-666; e-mail: crysdata@fiz-karlsruhe.de), on quoting the depository numbers CSD 418490 (Li_6PS_5Cl), CSD 418488 (Li_6PS_5Br), and CSD 418489 (Li_6PS_5I).

